Development and application of LED arrays for use in phototherapy research

Hadis, Mohammed; Cooper, Paul; Milward, Michael; Gorecki, Patricia; Tarte, Edward; Churm, James; Palin, William

DOI:
10.1002/jbio.201600273

Article type: Original article

The Development and Application of LED Arrays for use in Phototherapy Research

Mohammed A. Hadis[1 *], *Paul R. Cooper*[1], *Michael R. Milward*[1], *Patricia. C. Gorecki*[1], *Edward Tarte*[2], *James Churm*[2] *and William M. Palin*[1]

*Corresponding Author: E-mail: HadisM@bham.ac.uk

[1]School of Dentistry, College of Medical and Dental Sciences, Institute of Clinical Sciences, University of Birmingham, 5 Mill Pool Way, Edgbaston, Birmingham, B5 7EG, UK.
[2]School of Electronic, Electrical and Computer Engineering, University of Birmingham, Birmingham, B15 2TT, UK.

Keywords: photobiomodulation, phototherapy, photodisinfection, dentine-pulp complex, stem cells, low level light therapy

Abstract

Lasers/LEDs demonstrate therapeutic effects for a range of biomedical applications. However, a consensus on effective light irradiation parameters and efficient and reliable measurement techniques remain limited. The objective here is to develop, characterise and demonstrate the application of LED arrays in order to progress and improve the effectiveness and accuracy of *in vitro* photobiomodulation studies.

96-well plate format LED arrays (400-850nm) were developed and characterised to accurately assess irradiance delivery to cell cultures. Human dental pulp cells (DPCs) were irradiated (3.5-142mW/cm^2: 15-120s) and the biological responses were assessed using MTT assays.

Array calibration was confirmed using a range of optical and analytical techniques. Multivariate analysis of variance revealed biological responses were dependent on wavelength, exposure time and the post-exposure assay time ($P<0.05$). Increased MTT asbsorbance was measured 24h post-irradiation for 30s exposures of 3.5mW/cm^2 at 470, 527, 631, 655nm, 680, 777, 798 and 826nm with distinct peaks at 631nm and 798nm ($P<0.05$). Similar wavelengths were also effective at higher irradiances (48-142mW/cm^2).

LED arrays and high throughput assays provide a robust and reliable platform to rapidly identify irradiation parameters which is both time- and cost-effective. These arrrays are applicable in photobiomodulation photodynamic therapy and other photobiomedicine research.

1. Introduction

Phototherapy involves the application of light for the treatment of various medical conditions and can be broadly classified into two catagories, either photodynamic therapy (PDT) or 'low level light (laser) therapy' (LLLT) or the recently accepted, and more appropriately termed Medical Subject Heading (MeSH), 'photobiomodulation' (PBM). Whilst the beneficial effects of PDT are realised through an intermediatory photosensitizing step, PBM involves the application of low powered (<500mW), non-thermal, non-ablative light sources, predominantly lasers and light emitting diodes (LEDs), within the red to near infrared wavelength range ~600-1000nm to directly stimulate or inhibit cellular and biological processes. In either case, the therapeutic effects of light are attributed to the photophysical characteristics of the applied light, which include specific irradiation parameters such as wavelength, irradiance, exposure time and pulse frequency [1].

A significant number of articles have reported the beneficial effects of PBM in promoting tissue healing [2], reducing inflammation [3], reduceing oedema [4], restoreing blood flow [5] and induceing analgesia [6] in a range of healthcare areas, which include the treatment of musculoskeletal injuries [2] and neurodegenerative diseases such as rheumatoid arthritis [7]. The application of PBM has also been suggested in other healthcare areas which include the treatment of stroke and heart disease [8], macular degeneration [9] and dentistry [10-17].

Within a dental context, favourable data exists for oral health related conditions including oral mucositis [10], dentine hypersensitivity [11] candidiasis [12] and others [13]. Odontoblast-like cell modulation has also been reported which has significance for treatment of diseases such as dental caries [14-18]. Stimulation of the dentine-pulp complex has been shown to modulate oxidative stress [17] and promote natural repair processes through reactive oxygen species (ROS) activation of latent transforming growth factors (TGF-ß1). Subsequently,

activation of these processes reportedly triggers the differentiation of stem cells into odontoblast-like cells necessary for dental tissue regeneration [14-20].

Although beneficial clinical effects of PBM are commonly reported, the associated photophysics of light delivery remains poorly understood and mis-reported in a significant proportion of PBM publications. Undoubtly, this raises many questions about the reliability and reproducibility of such studies [1]; both of which are concerns in many areas of science [21]. These problems are further exacberated by the frequent reporting of incomplete, inaccurate, and unverified irradiation parameters with ambiguous or incorrect terminology despite several articles already emphasising their importance [1, 22]. There also currently exists no common consensus for the most effective irradiation parameters for any given PBM application. Consequently, data comparison between studies is often difficult and may have led to applications where light delivery is less than optimal, resulting in nil or false negative outcomes [23]. Such conculsions maybe ascribed to the existance of the Arndt-Schulz or hormesis curve [24] where too much or too little energy, as well as pulse structure and insufficient irradiation area [24-25] can result in non significant beneficial effects [25].

Whilst the irradiation parameters are a key component of PBM, their effects are also likely to be cell specific. PBM effects have been attributed to light absorption by mitochondria [27], therefore it may follow that cells with higher density of mitochondria will respond more favourably compared with cells that have less. Furthermore, the sensitivity of specific cell types to light may differ resulting in differences in biological response. Thus, it is likely that specific irradiation parameters would be required to optimize therapeutic effects in any given cell type.

The optimistaion of irradiation parameters to enhance PBM outcomes for specific cell types and a better understanding of biological processes maybe achieved through the screening of multiple irradiation and dosimetry parameters. In previous dose-response studies authors have

only investigated a limited number of wavelengths and irradiation parameters [17, 24, 28-30], which may be due to time, equipment availability and financial constraints. Some studies have utilised LED or laser arrays but where also limited by the number of wavelengths (12 x 785nm lasers [28], 24 x 855nm diodes [17] or 532nm and 630nm LEDs [29]). Similar devices have also been developed for PDT studies which have interchangeable heads that can target specific photosensitizers [30].

Consequently, the objective of this study was to develop multi-wavelength LED arrays and demonstrate the application of an *in vitro* high-throughput screening assay to rapidly identify enhanced irradiation parameters in specific cell types.

2. Materials and Methods

2.1. LED Array Development

LED arrays were designed using CADSoft's EAGLE software in a 96-microwell plate configuration with sixty-centrally located LEDs (5mm epoxy encased; Roithner Laserthek, Austria) of ten different peak wavelengths (400-830nm; n=6; Figure 1). The LEDs were located centrally within the 96-microwell plate to limit the effects of media evaporation from the outer wells during cell culture incubation; a phenomenom which could alter cell growth rates and is known as the 'edge effect' [31]. Laminated non-conductive substrate (FR4, 130mm x150mm) was used to print conductive copper tracks to form a printed circuit board (PCB) that connected the electrical components including resistors, LEDs, switches, voltage regulators and potentiometers, where applicable (these components varied depending on the board specifications and are described below). Initially, a narrow spectrum array was built that consisted of wavlengths centred around those that are typically utilised in PBM studies (660nm; 625-690nm, and 810nm; 780-820nm; n=6). Each channel was protected by a current limiting resistor, which restricted the current to the appropriate levels for each group of LEDs. The resistor value was calculated for each channel by dividing the expected voltage drop across the resistor by the total current drawn by the parallel combination of the six LEDs in that channel. The circuit was fabricated in-house as a single sided PCB of 1.6mm thick, glass-reinforced epoxy laminate FR4 substrate, with 1oz weight of copper and a nickel/gold surface finish. Since the array was desinged with only a single bank of current limiting resistors, irradiance control individually in each channel was not possible in this narrow spectrum array. A second broad spectrum LED array was designed and developed to incorporate a broader range of wavelengths (400-830nm). The circuit was set up to have a potential divider on each

channel to allow independent voltage control for each set of LEDs. A 500Ω trimming potentiometer was wired as a variable resistor (RS Electronics, UK), which provided a variable current to the LEDs in order to control light output (irradiance control). A bank of further resistors acted to limit the current for when the potentiometer resistance was set to zero, this allowed for safe operation of the device. The value of the limiting resistor was calculated by dividing the expected voltage drop across the limiting resistor by the maximum current drawn through the parallel combination of the six LEDs in that channel.

For each array, a bespoke sleeve was manufactured by removing the clear plastic base of black 96-well plates (Corning, Sigma-Aldrich, UK). Preliminary studies identified the effectiveness of sleeves manufactured from clear, white and black plates and found that sleeves made from black plates were more effective at reducing light bleeding between adjacent wells. Thus the prepared plates had two functions; firstly, to house the LEDs individually within the wells to limit the cross-contamination of light into adjacent wells; secondly to provide accurate concentric alignment for irradiation of culture plates placed directly above. A programmable bench top power supply (Iso-Tech, IPS-603, UK) was used to power the arrays using appropriate stable voltage and current.

2.2. LED Array Characterization

2.2.1. Spectral characterization

To accurately assess light delivery during *in vitro* cell culture irradiation, a second 96-well plate (Corning, Sigma-Aldrich, UK) was stacked directly above the bespoke sleeve with LEDs inset (5mm). The alignment was such that the wells of the upper plate were concentric with the wells of the lower sleeve. A fibre-based UV-Vis spectrometer was used to assess each LED for absolute spectral irradiance using a UV-Vis spectrometer (USB4000, Ocean Optics, UK; n=6). The spectrometer was coupled to a 200µm optical fibre and an opaline glass CC3 cosine corrector (3.9mm diameter of collection area; 6mm outer diameter; Ocean Optics, UK) which was calibrated to a National Institute of Standards and Technology (NIST) traceable light source (Mikropack DH2000/ Ocean Optics, UK). As the wells of the 96-well plate also had diameters of 6mm, it facilitated the insertion and reliable concentric alignment of the cosine corrector into the wells to accurately assess the irradiance delivered at the base of the well plate (i.e. at the cell culture surface). Spectral irradiance measurements (n=3) were made using Spectrasuite software (Ocean Optics, UK) for each LED and the absolute irradiance was determined by integration of spectral irradiance within the LED emission region.

The broad spectrum array was further optimized by calibrating the variable resistors (potentiometers) to regulate the voltage in each channel and achieve similar irradiances at each wavelength. The spectral irradiance was monitored in real-time through Spectrasuite software whilst adjusting the potentiometer screws, which in turn controlled the irradiance. The screws were adjusted until the highest common irradiance value was obtained for all sets of LEDs (~3.5mW/cm^2), which is similar to the irradiance utilized previously for DPCs [14].

2.2.2. Real-time irradiance measurements

Following spectral irradiance measurements, each LED was assessed to ensure a stable irradiance output over specific exposure times using a fibre-coupled UV-Vis spectrometer, as described previously. The spectrometer was set to measure the change in irradiance by integrating the peak areas of each LED. A high acquisition rate ($0.20s^{-1}$) was obtained by utilising the scope mode function of the software and the measured intensity counts were converted into irradiance values and percentage change from known absolute irradiance values. In addition to real-time irradiance measurements, the spectral outputs at the start and end of irradiation were also recorded to assess any spectral shifts with time.

2.2.3. Absorption measurements

A broadband Deuterium-Tungsten NIST traceable light source (Mikropack DH2000) was used to determine the absorption characteristics of the cell culture media (alpha MEM, Gibco, UK) and the clear plastic base of 96-well plates. The light was guided through an optical fibre (600μm) and passed through either air, an empty well of a 96-well plate, or a well containing 150μL of culture media before passing through a second optical fibre (600μm). The system was calibrated so that a 'light spectrum' was stored in the presence of an equivalent amount of PBS for the media measurements and the equivalent amount of 'air' for the measurement of the clear plastic base. A 'dark spectrum' was stored with the light source switched off to normalize the effect of ambient light.

2.2.3. Beam profile

Representative beam profile images of each of the LEDs were recorded using a silicon based CCD camera beam profiler (SP620, Ophir, Spiricon, Israel), which measured the spatial distribution of irradiance for each of the LEDs. The experimental set up was identical to that of the spectral irradiance measurements, i.e. the LEDs inset into the sleeve and a new 96-well plate placed on top. The CCD camera was equipped with a 50mm CCTV lens (Ophir, Spiricon, Israel) that was focused onto the clear plastic base of the plate corresponding to the LED that was under test. A maximum CCD sensor area was utilized by enlarging the beam image projected on the sensor by using spacer rings (Ophir, Spiricon; 20mm) between the sensor and lens to reduce the focal length. An optical scaling calibration was then applied to account for the enlarged image by measuring an object of known dimensions and calculating a scaling factor, which enabled pixel dimension calibration in the plane of the target screen. This process enabled precise linear measurement of the images and accurate beam diameter determination. Prior to beam imaging in each measurement, the system was corrected for ambient light and pixel response using the UltraCal function in Beam Gage Software (Ophir, Spiricon, Israel). Pre-determined power values (PD300 photodiode, Ophir Spiricon) were used for optical calibration. The diameter of the active light beam (D4σ or second moment width, ISO Reference 11145 3.5.2) was determined automatically by the Beam Gage software and was used to calculate the irradiance based on the input power values.

2.2.3. Thermal analysis

The thermal characteristics of each LED within the array were measured to ensure temperature was not a confounding factor in the biological response to light irradiation.

Sterile black 96-microwell plates with transparent bases were established containing 150µL of warm (37˚C) culture media to replicate culture conditions for *in vitro* tests. A K-type thermocouple (Maplin, UK; diameter 1.21mm) was embedded into a SubMiniature version A (SMA) adapter (6mm outer diameter, 4mm aperture) which allowed direct insertion of the thermocouple into the wells of the culture plate containing media. This ensured concentric and rigid alignment of the thermocouple within the well. The plate containing the media was aligned over the LED array and irradiated, replicating cell culture irradiation conditions (i.e. all LEDs switched on). The temperature was measured continuously (± 0.5˚C) at an acquisition rate of 2Hz for 120s through the multimeter device (Iso-Tech, IDM 207, UK) and logged through data capture software (Virtual DMM, UK). The change in temperature was calculated as the measured temperature minus initial temperature at t=0.

2.3. Biological Responses

2.3.1. Cell culture: Pulp cell isolation

Caries-free, intact wisdom teeth were obtained from Birmingham Dental Hospital following ethical approval from BBC CLRN RM&G Consortium Office (Approval number: BCHCDent334.1533.TB). Human dental pulp cells (DPCs) were isolated via the explant procedure [32] by removing the pulpal tissue, dissecting and homogenizing the tissue into small pieces and transferring into 25cm^2 culture flasks which were supplemented with 2ml of α-MEM (Biosera, UK)/20% fetal calf serum (FCS), 1% L-Glutamine and Amphotericin (1µL/ml). Cultures were incubated at 37˚C in a humidified atmosphere containing 5% CO_2 (Panasonic/MCO-18AC-PE, UK).

DPCs at passages 2-4 were trypsinised and re-suspended in phenol-red-free α-MEM (Gibco, UK)/10% FCS. Sixty centrally located wells of sterile black 96-microwell plates with transparent bases (Corning, Sigma-Aldrich, UK) were seeded with DPC suspension (150µL; 25,000 cell/ml). Seeded plates were incubated at 37˚C in a humidified atmosphere containing 5% CO_2 (Panasonic/MCO-18AC-PE, UK).

2.3.3. Irradiation of cultures

24h after seeding, cell culture plates were removed from the incubator and placed directly above the LED array in concentric alignment with the sleeve. This allowed alignment of the wells of the lower sleeve with the wells in the upper culture plate. Thus, the cultures were irradiated from directly beneath using the bespoke LED arrays for time intervals of up to 120s to represent exposure times within a clinically relevent timeframe. The specific irradiation parameters in terms of irradiance, and radiant exposure for each time interval at each wavelength are reported in Table 1. A full set of irradiation parameters are reported in Supplementary Table 1. 54 culture wells were irradiated simultaneously with one group of LEDs used as non-irradiated controls (n=6; Figure 1). Following irradiation, cultures were incubated until required for further anlysis.

2.3.4. 3-(4,5-Dimethyl thiazole-2-yl)-2,5-di-phenyl tetrazolium bromide (MTT) assay

Metabolic and mitochondrial activity was assessed via a modified 3-(4,5-Dimethyl thiazole-2-yl)-2,5-di-phenyl tetrazolium bromide (MTT) assay. An MTT solution containing 0.005g/ml of MTT reagent was made and aliquoted (15µL) into each culture well at 4h or 24h post-irradiation. The cultures where re-incubated for 4h at 37˚C. Following the final incubation

period, the media and MTT reagent were removed from the wells and subsequently 50µL of DMSO was added to the wells to solubilize the formazan crystals with gentle agitation for 10 mins. The absorbance of the resulting solution was determined at a wavelength of 570nm (ELx800 Universal Micro-plate reader, Bio-Tek Instruments, UK).

2.4. Statistical analysis

Statistically significant differences were identified using multi-factorial analysis of variance (ANOVA) and post-hoc Tukey comparisons (95% confidence level). The independent variables (exposure times, wavelength and time at which measurement was taken) were compared using General Linear Models (GLM) ANOVAs (P=0.05). Complimentary one-way ANOVAS and post-hoc Tukey comparisons were also performed to separate the differences (P=0.05).

3. Results and Discussion

3.1. Development and characterization of arrays for high-throughput analysis

LED arrays for *in vitro* phototherapy applications provide a relatively simple and unique platform to assess a multitude of parameters associated with light delivery that include wavelength, irradiance, exposure time, radiant energy and radiant exposure. Here, two LED arrays comprising of ten different wavelengths (n=6) were developed; one having a narrow range of wavelengths centered around those typically used in PBM studies (660nm and 810nm) [33-34] and the other with a broad range of wavelengths (400-850nm). Whilst other studies have previously compared the effect of different wavelengths for PBM [1, 33-34], there are no studies that have systematically compared an extensive range of wavelengths as reported here. Furthermore, in comparison to studies where array type light sources were used for specific purposes and targets [30], these arrays are not only applicable for *in vitro* PBM studies both at short and long wavelengths [35] but also applicable in a range of other research areas including PDT [30] and photodisinfection [17, 28-30]. In each case, the application and understanding of the photophysics of light is critical in order to understand the effects of dosimetry and any proceeding biological effect. Whilst some information of optical properties is available through manufacturers data sheets for LEDs, these are usually measured under ideal conditions which do not represent *in vitro* experimental conditions. The differences between manufacturers data and experimental data are certainly evident in Figure 2 where the measured peak wavelengths are not in agreement with manufacturers data (annotated Vs. legend respectively) Furthermore, there exists a wide intra- and extra- batch variations in terms of wavelength and power amongst similar light sources which is usually minimized by a process known as ‘binning’ by light source manufacturers. Here, a range of

optical-analytical techniques were employed to fully characterize the arrays within the remits of the experimental conditions employed during cell irradiation, in order to accurately assess the effects of dosimetry on relevant biological responses.

Whilst the arrays met the objective of providing a range of wavelengths within a narrow and broad range (Figure 2), significant differences in irradiance were measured for the various wavelengths in the narrow spectrum array ($P<0.05$). This was attributed to non-controllable irradiance in each channel and the maximum power outputs of the LEDs being wavelength dependent. However, the adjustable potentiometers of the broad range array allowed calibration to standardize the irradiance to achieve a baseline irradiance value of 3.5mW/cm^2 at each wavelength (Figure 2). This value was chosen since our previous study reported the stimulation of DPCs using red light emitting diodes (653nm) at similar irradiance [14] although other irradiances have also been shown to be effective [15-18] for DPC stimulation. Furthermore, a lower irradiance is likely to be more clinically relevant since attenuation by dental tissues will reduce the irradiance delivered to dental pulp cells [36]. The irradiance values (the integral of spectral irradiance) for each array are reported in Table 1.

Each array was further characterized in real-time to assess the stability of the delivered irradiance, since any fluctuation would obviously alter the radiant exposure (the product of irradiance and exposure time) and total energy delivered to cells [1]. These measurements confirmed that neither array was susceptible to significant changes in irradiance and wavelength over the exposure times utilized in this study and therefore accurate dosimetry was verified. The real time irradiance traces and additional radiometric data (peak wavelengths, absolute irradiance and full width half maximums) derived from the spectral irradiance graphs are reported as Supplementary Table 2.

Another important consideration for accurate light characterization is the beam profile of the light source since its distribution over a given area is usually non-homogenous [36]. LED

light sources commonly exhibit a Gaussian irradiance distribution with maximum exitance at the centre of the diode that decreases towards the beam profile edge. Such non-uniformity will result in spatial irradiance variation across the target area and more pronounced for larger surface areas (an effect that will increase with increasing distance between the light source and target). Non-uniform light irradiation is likely to affect biological responses and should be minimized where possible by using suitable optics such as lens and diffusers. However, in the current experiment, since the LEDs were appropriately matched and concentrically aligned within the wells of the cultureware plastic, any effect of non-homogenous light distribution were reduced. Nonetheless, 'Gaussian' irradiance distribution was apparent at all wavelengths and these could be considered when interpreting biological data (Figure 3).

Other confounding factors that can affect light delivery were also eliminated through spectral absorbance measurements of cell culture plasticware (base of micro-well plates) and the culture media used during the irradiation procedure. Although media containing phenol red has strong absorbance centered at 558nm, there is also weaker absorbance at other wavelengths that were utilized in the LED arrays (~280-600nm; Figure 4). The phenol-red free media also has weak absorbance within this range but no significant absorbance at 558nm as found in the media containing phenol-red. The weak absorbance that is common in both media is likely due to the different salts and FCS present in the media. Since cell cultures are adherent and are irradiated through the bottom of the plates to maintain sterility, it could be assumed that the media is unlikely to have any significant effect on the amount of light that is delivered to the cells. In addition, whilst the characterization methods take into consideration any reduction in irradiance due to the distance between the LED array and culture plate (5mm) and any potential absorbance by culutureware plastic, absorbance measurements further revealed no detectable absorbance due to the plastic between 400-850nm.

Since PBM is not a heat-based therapy, the LED arrays were also characterized for thermal output to abrogate any confounding effects of temperature. Heat energy can be transferred as infrared radiation, which can result in increased temperatures in biological systems. Low-powered LEDs are known to produce negligible or minimal heating during short-term operation, however, it may be possible that thermal effects are enhanced in multiple LED array devices. Temperature measurements revealed that the irradiation procedure did not significantly affect the culture temperatures since the measured temperature decrease for the irradiated groups exhibited similar characteristics to the non-irradiated control groups (Figure 5). Removal of cell cultures from the incubator resulted in a significant decrease in culture temperature due to lower ambient temperature. In view of the fact that there were no significant differences in temperature change for any of the wavelengths compared to a non-irradiated control, only minimal heating effects due to LED irradiation can be inferred. Therefore, it can be reasonably assumed that any thermal effects are a negligible factor in the photobiomodulatory effects reported here.

3.2. Application of LED arrays and high-throughput analysis

The second objective of this paper was met by using a combination of multiple wavelength LED arrays and the modified MTT assays to demonstrate the application of an *in vitro* high-throughput screening assay to rapidly identify enhanced irradiation parameters in HDPCs. The multivariate analysis revealed that the photobiomodulatory responses was dependent on wavelength, exposure time and the post-exposure assay time point ($P<0.05$) for both LED arrays. One-way ANOVAs and post-hoc Tukey comparisons revealed that 24h incubation periods following irradiation resulted in significant increases in MTT absorbance compared with 4h incubation periods (for the same exposure time and irradiances). In most cases

(except analgesic effects through neuronal blockade [6]), the effects of PBM are unlikely to be instantaneous and the mechanism by which beneficial effects are realized are through increases in cellular respiration and various other biological processes [14, 27]. The amount of formazan produced by the MTT in a given time is dependent upon the metabolic activity of cells and is proportional to the number of cells [37]. Since PBM effects are unlikely to be instantaneous, longer incubation periods after irradiation are likely to improve the assay detection ability to better differentiate between various irradiation parameters. However, this experimental variable can be optimized for specific cell types which will aid in a more effective identification of irradiation parameters. As no significant effects were measured at 4h, these data sets are reported in Supplementary Figure 2.

At 24h, significant increases in MTT absorbance were measured in a wavelength and exposure-time dependent manner ($P<0.05$). Whilst 30s exposures significantly increased MTT absorbance for both arrays (Figure 6), 60s exposures were only significantly effective for the broad spectrum array (400-850nm); further increasing exposure time for this array resulted in no significant effects (Figure 6b). Since the broad spectrum array was standardized to deliver equivalent irradiance regardless of wavelength, the irradiance levels delivered were relatively low compared with those of the narrow spectrum array (9-142mW/cm^2, 625-830nm), which delivered the maximum irradiance permissible by the design of that array. Thus, for the same exposure times, the radiant exposure, or dose (product of irradiance and exposure time) was significantly higher for the narrow spectrum array. Indeed, dose-dependency relationships within PBM literatures exist and biphasic dose-responses are well known [1, 3, 14, 24]. However, there currently exists no single study investigating the effect of multiple wavelength and dose within PBM literature. Although the broad spectrum array has the advantage of standardized irradiance to compare wavelength, in order to fully assess the effect of dose combinations, different irradiances and exposures times should be applied

to independently assess each parameter. Here the combination of data from the two arrays (albeit at different irradiances and radiant exposures) demonstrates the possibility to investigate such an effect in a rigorous and systematic manner.

In addition, whilst the broad spectrum array is standardized in terms of irradiance, the energy of the photons and the photonic flux (the number of photons delivered per square metre, which is a function of irradiance and wavelength) would differ between wavelengths. Therefore, even irradiance standardization would only give an estimation of wavelength and dose-dependency relationships. Equivalent photonic flux (albeit at different irradiances) could be calculated for each wavelength and irradiance values could be adjusted so that the same 'dose' is delivered as a function of wavelength with varying photon energy; a consideration that is currently overlooked in PBM studies.

HDPC cultures at relatively early passage, as those used here, are likely to be heterogeneous and contain stem/progenitor cells, endothelial cells and fibroblasts and hence may exhibit significant *in vivo* relevance [38]. Whist HDPCs have *in vivo* relevance; the individual cell types within this heterogeneous mixture may exhibit variable responses at specific wavelengths and doses [35, 39]. Effects of light irradiation could be further investigated in specific cell types to fully understand dosing relationships for specific purposes.

In the current study, significant increases in MTT absorbance were measured at multiple wavelengths (Figure 6). Although not significant, at 470nm (120s exposure), MTT absorbance was lower than all other groups. The cytotoxic effects of short wavelength UV light are well known and longer wavelength visible blue light (~400-500nm) is considered to be safer for human cells [40]. Whilst in the current study, the effects at 470nm where non-significant, these LED arrays could also be used to identify harmful wavelengths and irradiation parameters to minimize risks when applied *in vivo*.

Other biological assays such ATP and NO assays [14] can also be applied to identify effective irradiation parameters [14, 17] using the proposed irradiation method. However, the MTT assay is a relatively inexpensive and a rapid solution due to the almost instantaneous reaction through reduction of the MTT dye by the enzyme succinate dehydrogenase, thus allowing rapid high-throughput analysis of biological effects. Similar assays have been used in other PBM studies to identify effective irradiation parameters and have been shown to correlate with increased NO and ATP production as well as other signaling molecules such as growth factors and reactive oxygen species leading to increased cell proliferation [14, 17]. The success of this high-throughput assay is underpinned by the development of the LED arrays and the subsequent characterization and calibration to accurately deliver light. These developments present a novel method that can be used to systematically and rigorously investigate various irradiation parameters in a range of cell types to assess PBM and photocytotoxic effects. It may further be possible to investigate the spectral quantum efficiency of applied light to provide a better insight into PBM mechanisms.

4. Conclusion

LED arrays were developed, characterized and then applied to identify effective irradiation parameters for HDPC stimulation. The optimization of the technique allowed increased MTT absorbance to be measured 24h post-irradiation for 30s exposures of 3.5mW/cm^2 at 470, 527, 631, 655nm, 680, 777, 798 and 826nm with distinct peaks at 631nm and 798nm. The development and application of LED arrays and high throughput assays provide a robust and reliable platform to rapidly identify irradiation parameters which is both time- and cost-effective. These arrays can be used to identify effective or optimised irradiation parameters in a range of cell types and the spectral quantum efficiencies for various PBM applications. Furthermore, these arrrays are also applicable in other photomedicine research areas such as photodynamic therapy and photocytotoxicty screening.

Supporting Information

Additional supporting information may be found in the online version of this article at the publisher's website.

Figure S1: The real time irradiance measured to assess fluctuations in irradiance during the irradiation procedure. The charts show no significant changes in irradiance over the exposure times used thus confirming accurate delivery of irradiance and radiant exposure.

Figure S2: Percentage changes in MTT absorbance of irradiated compared to non-irradiated control groups measured 4hrs after irradiation. No significant differences were identified through One-Way ANOVAs and post-hoc Tukey comparisons ($P<0.05$).

Figure S3: Percentage changes in MTT absorbance of irradiated groups compared to non-irradiated control groups measured 24hrs after irradiation for the narrow spectrum array. * represent significant increases in MTT absorbance assessed through One-Way ANOVAs and post-hoc Tukey comparisons ($P<0.05$).

Figure S4: Percentage changes in MTT absorbance of irradiated groups compared to non-irradiated control groups measured 24hrs after irradiation for the broad spectrum array. * represent significant increases in MTT absorbance assessed through One-Way ANOVAs and post-hoc Tukey comparisons ($P<0.05$).

Supplementary Table 1: Specific wavelengths, irradiance and radiant exposures delivered to cell cultures using each of the arrays for the full set of exposure times utilized in this study.

Supplementary Table 2: The radiometric data derived from the spectral irradiance graphs which confirm accurate delivery of irradiance and wavelengths.

Acknowledgements

This report is independent research funded by the National Institute for Health Research (Invention for Innovation (I4I), Product Development Awards, II-LB-0712-20003). The views expressed in this publication are those of the author(s) and not necessarily those of the NHS, the National Institute for Health Research or the Department of Health.

Author Biographies Please see Supporting Information online

Dr Mohammed Hadis – Research fellow, School of Dentistry, University of Birmingham. His research interests and expertise relates to biomedical applications of lights from photo-curing of composite materials to interaction of light with cells, tissue, molecules and micro-organisms. He provides key skills in the field of photonics for the development of novel technologies and currently working on projects funded by the National Institute of Health Research and The Ministry of Defence. His research has been awarded several prestigious awards including the Paffenbarger Award for outstanding research and the Heraeus Kulzer Award for innovative testing design.

Professor Paul Cooper received his PhD from the University of Birmingham, UK in Cancer Sciences in 1995. He has worked as a post-doctoral researcher at Roswell Park Cancer Institute, New York, US and for Novartis Pharmaceuticals, UK. He conducts research into stem cells, immune/inflammation and tissue regeneration in oral and dental disease and the biomaterials area. He received the prestigious Young Investigator Award from the International Association for Dental Research in 2010. He has >100 full publications and attracted >£3-million research funding. He is currently the Director of Research at the School of Dentistry and leads the Oral Biology teaching.

Dr Mike Milward - *(Senior Clinical Lecturer / Honorary Consultant in Periodontology, School of Dentistry)*
Initially trained/qualified as a microbiologist before embarking on undergraduate dental training, following completion he embarked a PhD investigating the role of bacteria in host inflammatory response. His research expertise relates to optimising approaches for the management of inflammation, infection and tissue repair. He has attracted in the region of £1.9-million in research funding. He is also a calibrated clinical examiner for over 12 clinical trials undertaken over the last 15 years investigating the clinical efficacy of a wide range of oral healthcare products.

Dr Patricia Gorecki - *(Academic Clinical Lecturer in Oral Surgery, School of Dentistry)*
Currently undertaking her specialty training in oral surgery. Following her undergraduate dental training, she was involved in Cancer Research, evaluating potential molecular markers for assessing the malignant potential of oral premalignant lesions, for which she also received her doctorate degree. After joining the University of Birmingham, her main research focus has been in clinical research, based on evaluation of pain following third molar surgery.

James Churm is a Ph.D. student at the University of Birmingham looking into the development of novel neural interface technologies in the School of Engineering. James graduated with MEng(Hons) in Electronic and Computer Engineering from the University of Birmingham in 2012 and since then he has been studying under Dr Edward Tarte and is interested in biological and novel applications for engineering principles.

Dr Edward Tarte is a Senior Lecturer in the School of Engineering at the University of Birmingham. He graduated in 1988 with an BSc(Hons) in Physics from the University of Bristol and went on to study for a PhD in the physics of superconducting devices at the University of Cambridge. He worked on superconducting devices in Cambridge until 2005 where he investigated the use of Superconducting Quantum Interference Devices (SQUIDs) to detect neuronal activity in-vitro. Edward moved to Birmingham in 2005 as a University Research Fellow, where his interest in the detection of bioelectric phenomena became the core of his research program. His team developed an electrical interface for the peripheral nervous system, in collaboration with colleagues in Cambridge and King's College in London, for which a patent reached the international stage. He is more generally interested in the applications of biomedical electrical engineering and the biomedical applications of electronics. He has been funded by the UK EPSRC, the UK MOD, the EU Framework programme, the Royal Society and the British Council. He was elected a Fellow of the UK Institute of Physics in 2008.

Professor William M Palin (Professor and Chair in Biomedical Materials Science, University of Birmingham) has an international reputation in the biomaterials field and an established track record in managing research grants at the materials engineering-biological interface. His specific research expertise lies in the development of novel biomaterial devices and relevant technologies, which includes light source and fibre optic light delivery design for light-curable restorative and therapeutic dental and medical materials. Dr Palin is joint founder of the Photonics Research Group at the University of Birmingham and has attracted over £1.3 million of research funding from research councils, UK charities and industry.

References

[1] M.A. Hadis, S.A. Zainal, M.J. Holder, J.D. Carroll, P.R. Cooper, M.R. Milward and W.M. Palin, "The dark art of light measurement: accurate radiometry for low-level light therapy," *Lasers Med Sci*, **31,** 789-809 (2016)

[2] J.T. Hopkins, T.A. McLoda, J.G. Seegmiller, and D.G. Baxter,"Low-Level Laser Therapy Facilitates Superficial Wound Healing in Humans: A Triple-Blind, Sham-Controlled Study," *J Athl Train* **39**, 226-229 (2004)

[3] F. Aimbire, R. Albertini, M.T.T. Pacheco, H.C. Castro-Faria-Neto, P.S.L.M. Leonardo, V.V. Iversen, L. Martins, and J.M. Bjordal, "Low-level laser therapy induces dose-dependent reduction of TNFalpha levels in acute inflammation," *Photomed Laser Surg* **24,** 33-37 (2006)

[4] A. Stergioulas, "Low-Level Laser Treatment Can reduce Edema In Second Degree Ankle Sprains," *J Clin Laser Med Surg* **22**, 125-128 (2004)

[5] P. Avci, A. Gupta, M. Sadasivam, D. Vecchio, Z. Pam, N. Pam, M.R. Hamblin, "Low-level laser (light) therapy (LLLT) in skin:stimulating, healing and restoring, " *Sermin Cutan Med Surg* **32,** "41-52 (2013)

[6] J.D. Kingsley, T. Demchak, R. Mathis, "Low-level laser therapy as a treatment for chronic pain," *Front Physiol* **5,** 306 (2014)

[7] L. Brosseau, V. Welch, G. Wells, P. Tugwell, R. de Bie, A. Gam, K. Harman, B. Shea, and M. Morin M, "Low level laer therapy for osteoarthritis and rheumatoid arthritis: a metaanalysis," *J Rheum* **27**, 1961-1969 (2000)

[8] T. Agrawal, G.K. Gupta, V. Rai, J.D. Carroll and M.R. Hamblin, "Pre-conditioning with low-level laser (light) therapy: light before the storm," *Dose Response* **12,** 619-649 (2014)

[9] B.T. Ivandic, T. Ivandic, "Low-level laser therapy improves vision in patients with age-related macular degeneration," *Photomed Laser Surg* **26,** 241-245 (2008)

[10] R.J. Bensadaun and R.G. Nair, "Efficacy of Low-Level Laser Therapy (LLLT) in Oral Mucositis: What Have We Learned from Randomised Studies and Meta-Analyses," *Photomed and Laser Surg* **30**, 191-192 (2012)

[11] R. Umberto, R. Claudia, P. Gaspare, T. Gianluca, and D.V. Alessandro, "Treatment of dentine hypersensitivity by diode laser: a clinical study," Dentistry **2012**: 858950 (2012)

[12] F.G. Basso, C.F. Oliveira, A. Fontana, C. Kurachi, V.S. Bagnato, D.M. Spolidório, J. Hebling, and C.A. de Souza Cost, " In Vitro effect of low-level laser therapy on typical oral microbial biofilms," *Braz Dent J* **22**, 502-510 (2011)

[13] M.R. Milward, M.J. Holder, W.M. Palin, M.A. Hadis, J.D. Carroll, and P.R. Cooper, "Low level light therapy (LLLT) for the treatment and management of dental and oral diseases," *Dent Update* **41**, 763-772 (2014)

[14] M.J. Holder, M.R. Milward, W.M. Palin, M.A. Hadis, and P.R. Cooper, "Effects of red light-emitting diode irradiation on dental pulp cells," *J Dent Res* **91**, 961-966 (2012)

[15] P.R. Arany, A. Cho, T.D. Hunt, G. Sidhu, K. Shin, E. Hahm, G.X. Huang, J. Weaver, A.C. Chen, B.L. Padwa, M.R. Hamblin, M.H. Barcellos-Hoff, A.B. Kulkarni, and J.D Mooney, "Photoactivation of endogenous latent transforming growth factor-ß1 directs dental stem cell differentiation for regeneration," *Sci Transl Med* **6**, 238ra69 (2014)

[16] A.P.S. Turrioni, F.G. Basso, L.A. Montoro, L.F.D de Almeida, C.A. de Souza Costa, and J. Hebling, "Phototherapy up-regulates dentine matrix proteins expression and synthesis by stem cells from human-exfoliated deciduous teeth," *J Dent*, **42**, 1292-1299 (2014)

[17] L.A. Montoro, A.P.S. Turrioni, F.G. Basso, C.A. de Souza Costa and J. Hebling, "Infrared LED irradiation photobiomodulation of oxidative stress in human dental pulp cells," *Int Endo J* **47,** 747-755 (2014)

[18] L de F.D. de Almeida, A.P. Turrioni, F.G. Basso and L. Hebling, "Red LED photobiomodulates the metaboloic activity of Odontoblast-like cells," *Braz Dent J* **27**, 375-380 (2016)

[19] A. Ballini, F. Mastrangelo, G. Gastaldi, L. Tettamanti, N. Bukvic, S. Cantore, T. Cocco, R. Saini, A. Desiate, E. Gherlone and S. Scacco, "Osteogenic differentiation and gene expression of dental pulp cells under low-level laser irradiation: a good promise for tissue engineering," *J Biol Regul Homeost Agents* **29**, 813-822 (2015)

[20] M.T. Pagin, F.A. de Oliveira, R.C. Oliveira, A.C. Sant'Ana, M.L. de Rezende, S.L. Greghi and C.A. Damante, "Laser and light-emitting diode effects on pre-osteoblast growth and differentiation," *Lasers Med Sci*, **29**, 55-9 (2014)

[21] "A reality check on reproducibility," *Nature*, **533,** 437 (2016)

[22] P.A. Jenkins, J.D. Carroll, "How to report low-level laser therapy (LLLT)/photomedicine dose and beam parameters in clinical and laboratory studies," *Photomed Laser Surg* **29,** 785-787 (2011)

[23] A. Kansal, N. Kittur, V. Kumbhojkar, K.M. Keluskar, P. Dahiya, "Effect of low intensity laser therapy on the rate of orthodontic tooth movement: a clinical trial," *Dent Res J (Isfahan)* **11,** 481-488 (2014)

[24] Y.Y. Huang, A.C.H. Chen, J.D. Carroll, and M.R. Hamblin, "Biphasic dose response in low level light therapy," *Dose response* **7**, 358-383 (2009)

[25] J. Tunér and L. Hode, "It's All in the Parameters: A critical Analysis of some Well-Known Negative Studies on Low-Level Laser Therapy," *J Clin Laser Med and Surg* **16**, 245-248 (1998)

[26] S. Ilic, S. Leichliter, J. Streeter, A. Oron, L. DeTaboada, and U. Oron, "Effects of Power Densities, Continuous and Pulse Frequencies, and Number of Sessions of Low-level Laser Therapy on Intact Rat Brain," *Photomed Laser Surg* **24**, 458-466 (2006)

[27] T.I. Karu and S.F. Kolyakov, "Exact action spectra for cellular responses relevant to phototherapy," *Photomed Laser Surg* **23**, 355-361 (2005)

[28] E.C. Lins, C.F. Oliveira, O.C.C. Guimarães, C.A. de Souza Costa, C. Kurachi, and V.S. Bagnato, "A novel 785-nm laser diode-based system for standardization of cell culture irradiation," *Photomed Laser Surg* **10**, 466-473 (2013)

[29] S.D. Soltani, A. Babaee, M. Shojaei, P. Salehinejad, F. Seyedi, M.J. Kamali and S.N. Nematollahi-Mahani, "Different effects of energy dependent irradiation of red and green lights on proliferation of human umbilical cord matrix-derived mesenchymal cells," *Lasers Med Sci*, **31**, 255-261 (2016)

[30] F.L.E. Florez, M.C.G. Del Arco, S.L. de Souza Salvador, V.S. Bagnato and O.B.O. Jùnior OBO. "Viability study of antimicrobial photodynamic therapy using curcumin, hypercin and photogem photosensitizers in planktonic cells of *streptococcus mutans*," *Dent* **2**, 22-27 (2015)

[31] A. Walzl, N. Kramer, G. Mazza, M. Rosner, D. Falkenhagen, M. Hengstschläger, D. Schwanzer-Pfeiffer and H. Dolznig, "A simple and cost efficient method to avoid unequal evaporation in cellular screening assays, which restores metabolic activity," *I J App Sci Tech* **2**, 17-25 (2012)

[32] O. Cortes, C. Garcia, L. Perez, J. Boj, and A. Alcaina, " Pulp cell cultures obtained with two different methods for in vitro cytotoxicity tests," *Eur Arch Paediatr Dent* **7**, 96-99 (2006)

[33] H. Chung, T. Dai, S.K. Sharma, Y.Y. Huang, J.D. Carroll, and M.R. Hamblin, "The nuts and bolts of low-level (light) therapy," *Amm Biomed Eng* **40**, 516-533 (2012)

[34] A.S. de Rosa, A.F. Dos Santos, M.M. da Silva, G.G. Facco, D.M. Perreira, A.C. Alves, E.C. Leal Junior, and P.T. de Carvalho, "Effects of low-level laser therapy at wavelengths of 660 and 808nm in experimental model of osteoarthritis," *Photochem Photobiol* **88**, 161-166 (2012)

[35] A. Gupta, P. Avci, T. Dai, Y.Y. Huang, and M.R. Hamblin, "Ultraviolet Radiation in Wound Care: Sterilization and Stimulation," *Adv Wound Care* **2**, 422-437 (2013)

[36] W.M. Palin, M.A. Hadis, M.R. Milward, J.D. Carroll and P. R. Cooper,"Beam profile measurements for dental phototherapy: the effect of distance, wavelength and tissue thickness," *Proc. SPIE 9309, Mechanisms for low-level light therapy X* **930905** (2015): doi: 10.1117/12.2077628

[37] D.M.L. Morgan, "Tetrazolium (MTT) Assay for Cellular viability and Activity," *Methods in Molecular Biology*, **79**, 179-183

[38] M. Patel, A.J. Smith, A.J. Sloan, G. Smith, and P.R. Cooper, "Phenotype and behaviour of dental pulp cells during expansion culture," *Arch Oral Biol* **54**, 898-908 (2009)

[39] J. Liebmann, M. Born and V. Kolb-Bachofen, " Blue-light irradiation regulates proliferation and differentiation in human skin cells," *J Invest Dermatol* **130**, 259-269 (2010)

[40] Y. Matsumura and H,N. Ananthaswamy, "Toxic effects of ultraviolet radiation on skin," *Toxicology and Applied Pharmacology* **195,** 298-308 (2004)

Figure 1. Image and schematic representations of the LED arrays. In each array, columns 1 and 12, and rows A and H were not used as the outer wells may be more susceptible to media evaporation which is known to effect biological outcomes. Shaded areas within the schematic diagrams represent the active areas were cells were cultured and irradiated at specific wavelengths.

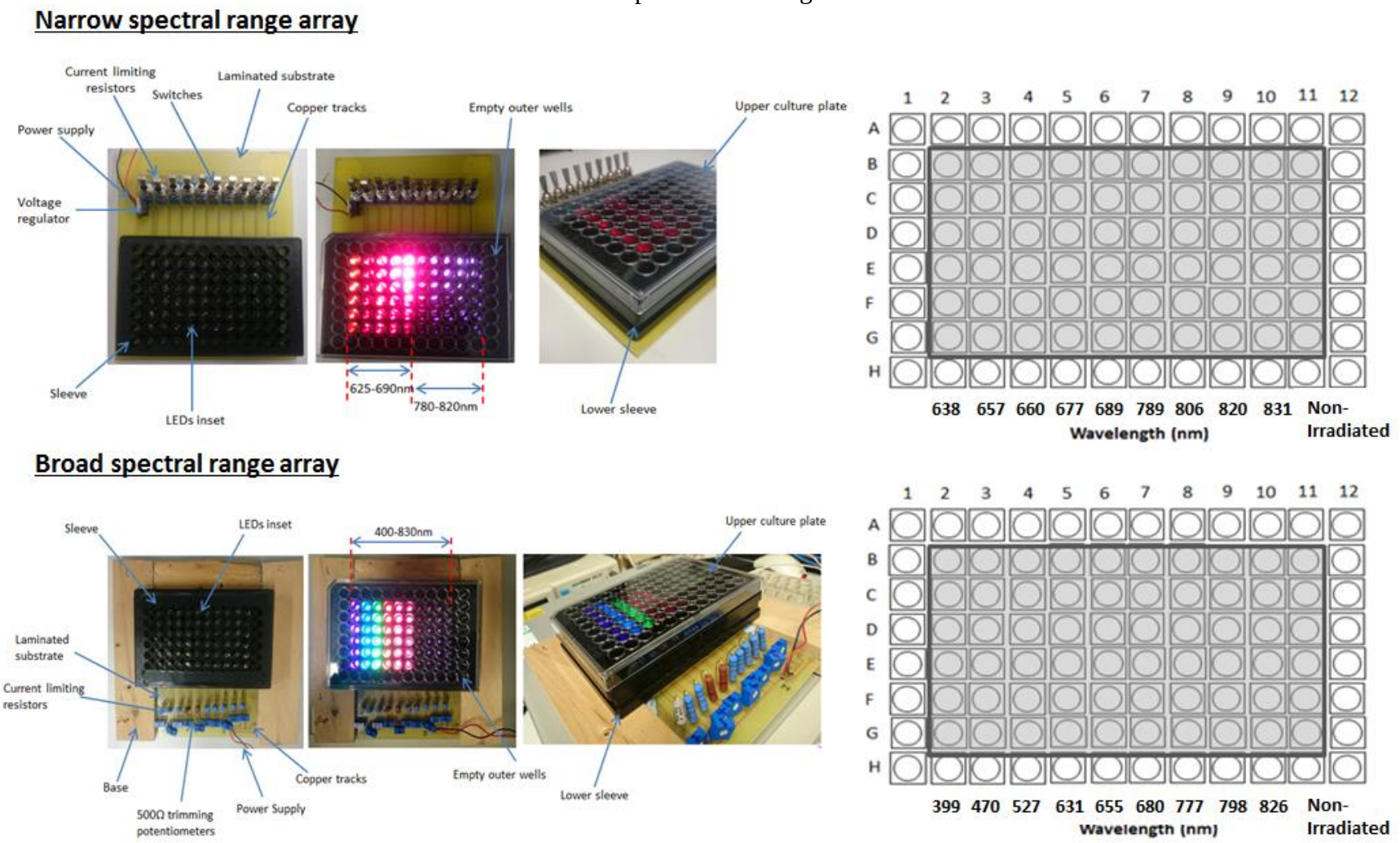

Figure 2. The spectral irradiance of the LEDs measured using a fibre-coupled UV-Vis spectrometer. For the broad spectrum array, spectral irradiance was re-measured following irradiance standarisation. The integral of the peaks represent the absolute irradiance emitted by each set of LEDs (these values can be found in the supplementary data section).

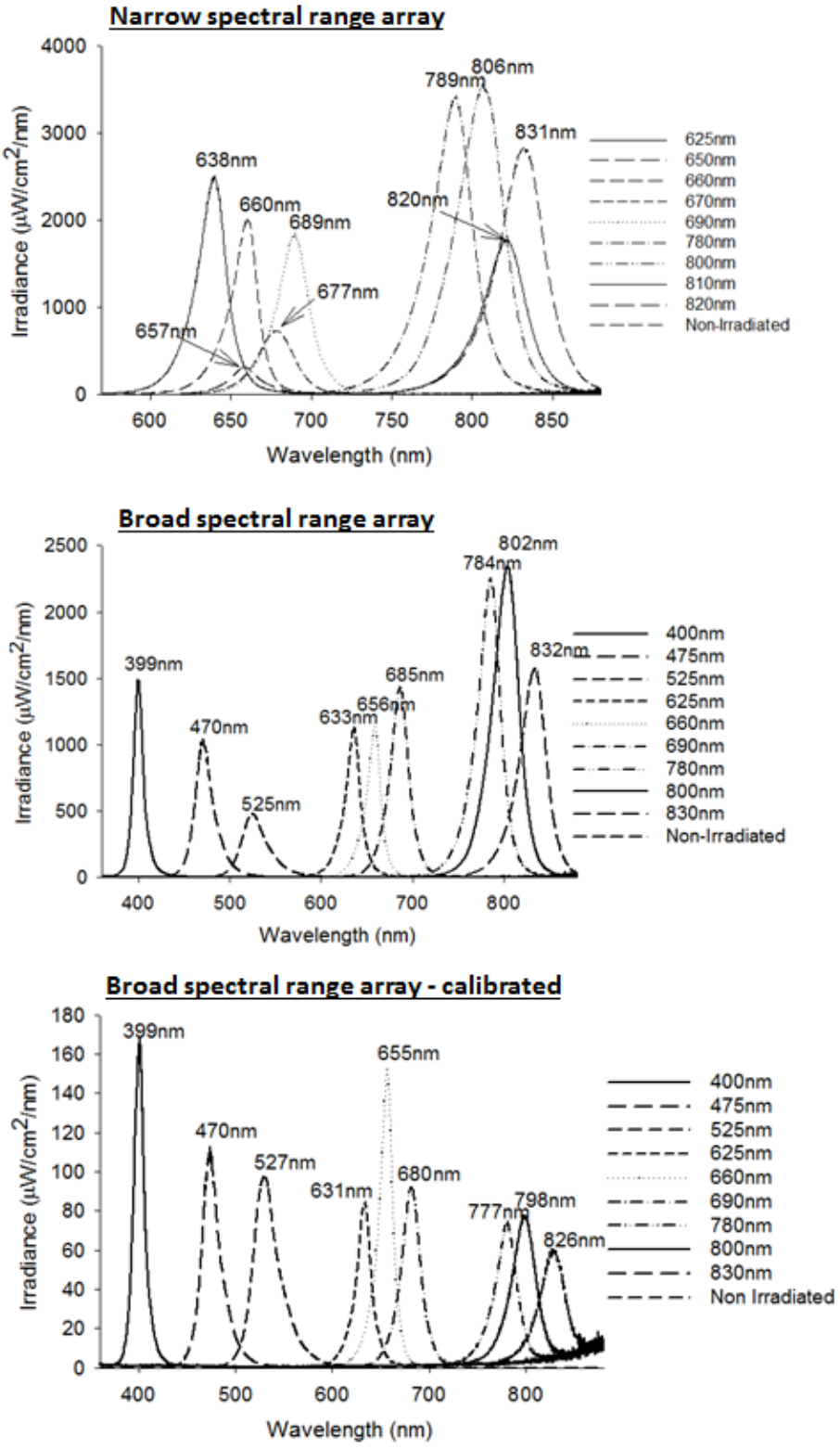

Figure 3. The beam profile images showing the distribution of irradiance across the culture surfaces of 96-well plates. Whilst there is a 'Gaussian' distribution in irradiance, the LEDs are appropriately matched to irradiate the full culture areas.

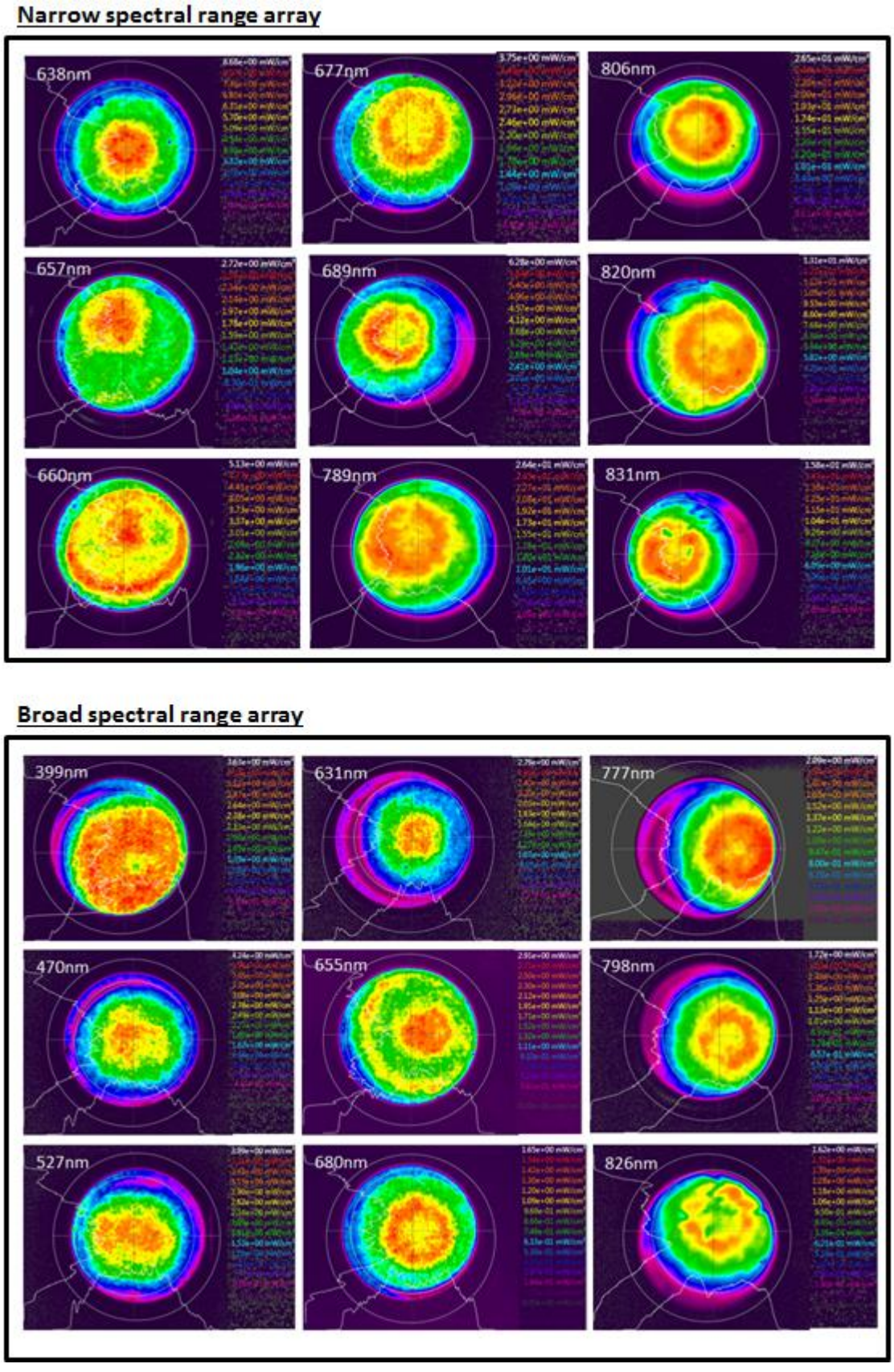

Figure 4. The absorption profiles of the media used to culture cells and the absorption profile of the base of the micro-well plate for which light penetrates to reach cells during irradiation.

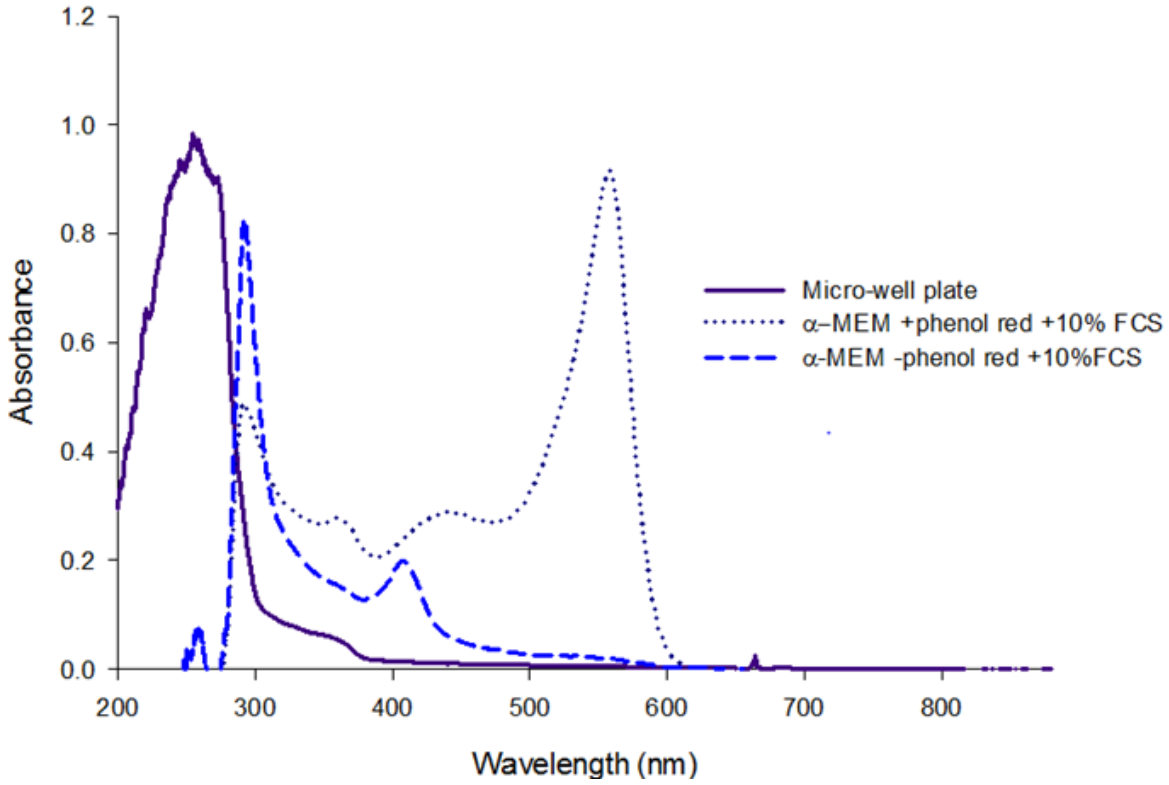

Figure 5. The temperature change during irradiation following immediate removal from 37˚C incubator.

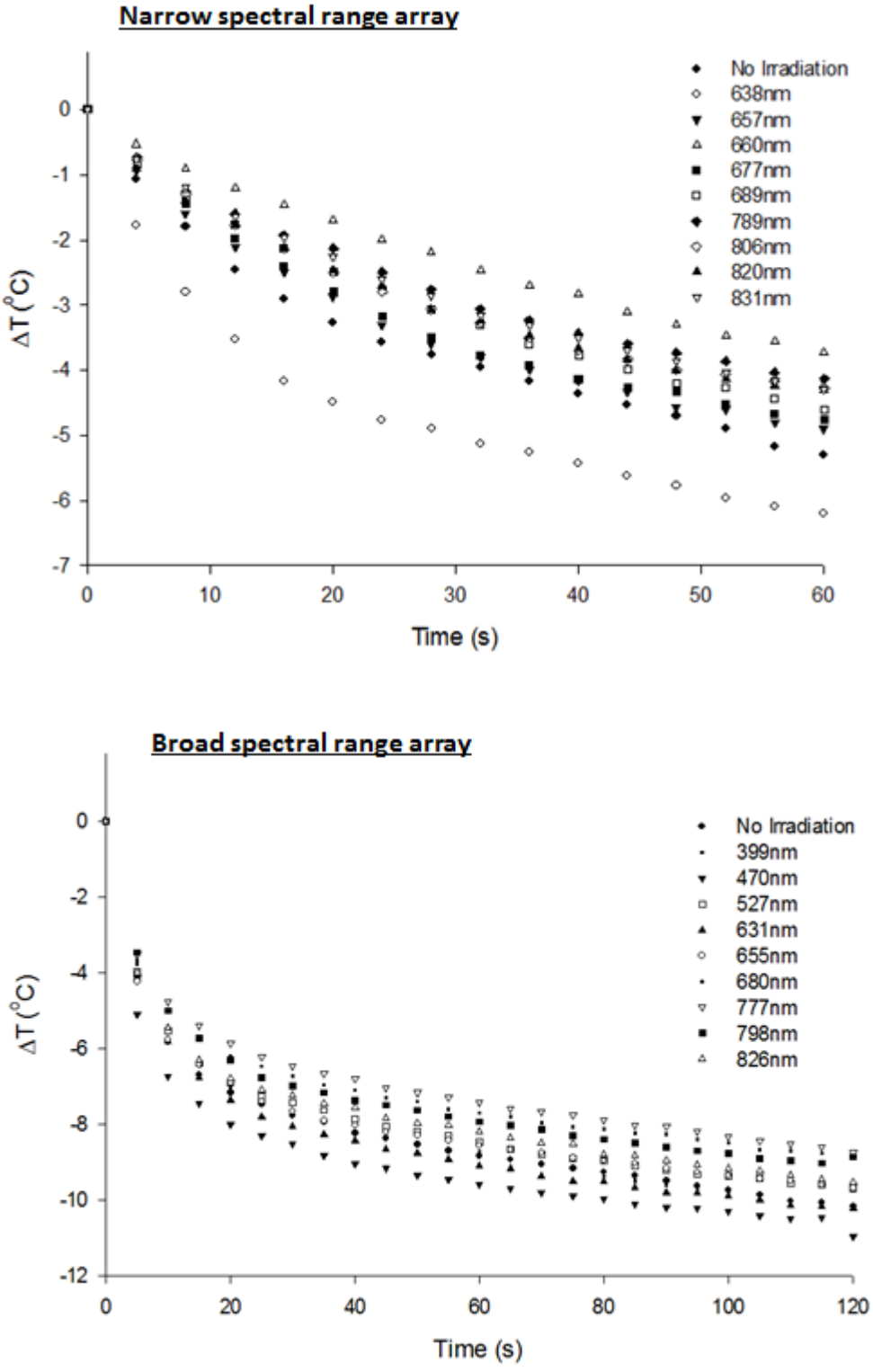

Figure 6. Percentage changes in MTT absorbance of irradiated groups at selected exposure times compared to non-irradiated control groups measured 24h after irradiation. * represent significant increases in MTT absorbance assessed through One-Way ANOVAs and post-hoc Tukey comparisons ($P<0.05$). The full set of data can be found in the supplementary information section.

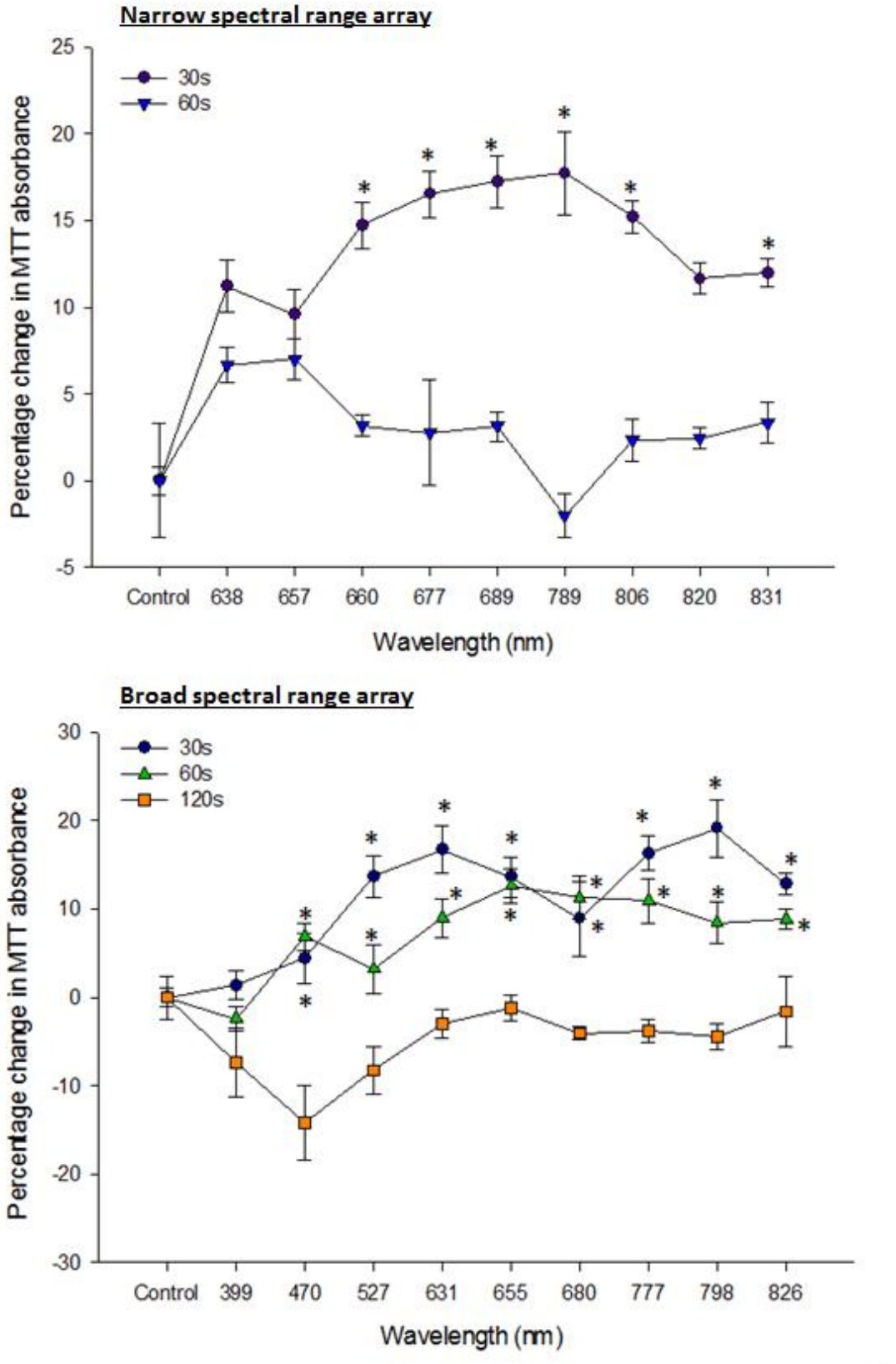

Table 1. Specific wavelengths, irradiance and radiant exposures delivered to cell cultures using each of the arrays.

Narrow spectral range array

Wavelength (nm)	Irradiance (mW/cm^2)	Radiant exposure at 30s (J/cm^2)	Radiant exposure at 60s (J/cm^2)
638 ± 2	66 ± 11	1.98	3.96
657 ± 1	9 ± 1	0.27	0.54
660 ± 0	48 ± 2	1.44	2.88
677 ± 4	23 ± 2	0.69	1.38
689 ± 3	52 ± 14	1.56	3.12
789 ± 1	126 ± 15	3.78	7.56
806 ± 3	142 ± 33	4.26	8.52
820 ± 2	67 ± 13	2.01	4.02
831 ± 2	114 ± 16	3.42	6.84

Broad spectral range array

Wavelength (nm)	Irradiance (mW/cm^2)	Radiant exposure at 30s (J/cm^2)	Radiant exposure at 60s (J/cm^2)	Radiant exposure at 120s (J/cm^2)
399 ± 1	3.46 ± 0.40	0.10	0.21	0.42
470 ± 1	3.86 ± 0.50	0.12	0.23	0.46
527 ± 0	3.59 ± 0.69	0.11	0.22	0.43
631 ± 4	3.36 ± 0.22	0.10	0.20	0.40
655 ± 3	3.91 ± 0.70	0.12	0.23	0.47
680 ± 1	3.55 ± 0.34	0.11	0.21	0.43
777 ± 3	3.30 ± 0.16	0.10	0.20	0.40
798 ± 2	3.59 ± 0.54	0.11	0.22	0.43
826 ± 2	3.03 ± 0.43	0.09	0.18	0.36
AVERAGE	**3.52 ± 0.27**	**0.11 ± 0.01**	**0.21 ± 0.02**	**0.42 ± 0.03**